

Smartphone-assisted Colorimetric Sensing Platform Based on Au@Pt Nanozyme Used for Visual Monitoring of Ascorbic Acid

Laixin Gao* and Lingchun Li

School of Chuzhou University,
No. 1 Huifeng West Road, Langya District, Chuzhou City, Anhui Province 239000, China

(Received February 20, 2024; accepted April 4, 2024)

Keywords: Au@Pt NPs, peroxidase-like nanozyme, ascorbic acid, colorimetric sensing, smartphone

Ascorbic acid (AA) is a vitamin similar to glucose polyol and is involved in various physiological and biochemical processes in the human body. Therefore, it is crucial to develop a quick and easy method for identifying AA to assess the freshness and nutritional value of fruits. In this study, we synthesized a novel Au@Pt nanoparticle structure, which exhibited excellent peroxide-like activity, by a one-step method. A colorimetric sensor for AA detection was then constructed on the basis of the chromogenic system of a nanoenzyme and 3,3',5,5'-tetramethylbenzidine (TMB). This colorimetric sensor had a low detection limit of 0.213 μM and showed a good linear relationship in the concentration range of 5 to 345 μM . By integrating this sensor with a smartphone-connected visual sensing platform using test paper, we enabled a quick, portable, and accurate visual monitoring of AA in fruits. In this work, we not only introduced a smartphone-assisted colorimetric sensor and a new and effective noble metal nanozyme, but also proposed a creative design approach for developing an inexpensive, user-friendly, and highly sensitive vitamin detection instrument.

1. Introduction

Ascorbic acid (AA), also known as vitamin C, is an essential water-soluble vitamin that plays a vital role in various physiological functions. It promotes collagen synthesis, which aids in tissue wound healing,^(1,2) is involved in the metabolism of amino acids such as tyrosine and tryptophan, and helps prolong the lifespan of cells.^(3,4) Since humans cannot produce AA on their own, it is commonly added as a supplement in beverages, food products, and medicines to improve their quality and promote human health.^(1,2) Therefore, the accurate detection and measurement of AA are of significant importance in ensuring food safety and diagnosing certain diseases.

Several approaches, including liquid chromatography,^(3,4) chemiluminescence,^(5,6) and electrochemical^(7,8) methods, have been developed thus far for the detection of AA. These techniques are expensive to run and highly complex. Colorimetry is preferred over other technologies because of its rapid detection, on-site analysis, and visual identification

*Corresponding author: e-mail: glx0411@126.com
<https://doi.org/10.18494/SAM5028>

capabilities.^(9–11) In particular, colorimetric sensors based on nanoscale materials, also known as nanozymes, have become significant colorimetric instruments.

Since the discovery of the distinctive peroxidase-like activity of Fe_3O_4 ⁽¹²⁾ nanoparticles, nanozymes, a novel class of nanomaterials exhibiting enzyme mimic activity, have attracted significant attention across a wide range of disciplines. Many of the typical drawbacks of natural enzymes, including their high cost, difficulty of purification, and low stability, can be addressed using nanozymes.⁽¹³⁾ Numerous nanozymes, including metal oxides,⁽¹⁴⁾ metal organic frameworks,⁽¹⁵⁾ carbon-based nanozymes,⁽¹⁶⁾ metal sulfides,⁽¹⁷⁾ and others,⁽¹⁸⁾ have been developed and used to catalyze enzymatic reactions thus far. Multicomponent core/shell nanoparticles, including Au@Pt nanoparticles, have attracted significant interest and have been employed as colorimetric indicators in place of peroxidase. Wu *et al.*⁽¹⁹⁾ developed a Au@Pt nanozyme-mediated magnetic relaxation conversion (MRS) DNA biosensor for the rapid detection of *Listeria monocytogenes*. The limit of detection (LOD) of this biosensor for *Listeria monocytogenes* is 30 CFU/mL. Bonet-Aleta *et al.*⁽²⁰⁾ synthesized a Au@Pt nanoparticle with a core-shell structure, which can detect and quantify GSH up to μM order, and its LOD was 34 nM. Xia *et al.*⁽²⁵⁾ reported Au@Pt composite nanoparticles (Au@Pt NPs) with high catalytic activity formed without using a reducing agent. They showed the linear detection of H_2O_2 in a wide concentration range of 0.5 to 1000 μM , and the LOD was as low as 0.11 μM .

In this work, we built a smartphone-based colorimetric sensor that uses Au@Pt NPs to instantly identify AA in fruits. The basis for this colorimetric sensing is the oxidation of 3, 3', 5, 5'-tetramethylbenzidine (TMB) to blue TMB (TMB_{ox}) in the absence of hydrogen peroxide, which is catalyzed by Au@Pt NPs with oxidase mimic activity. Through the single electron transfer process, AA with antioxidant properties can reduce TMB_{ox} to TMB and produce obvious blue discoloration (Fig. 1). We have developed a multimodal detection and analysis method that increases the number of application scenarios and boosts the accuracy of the

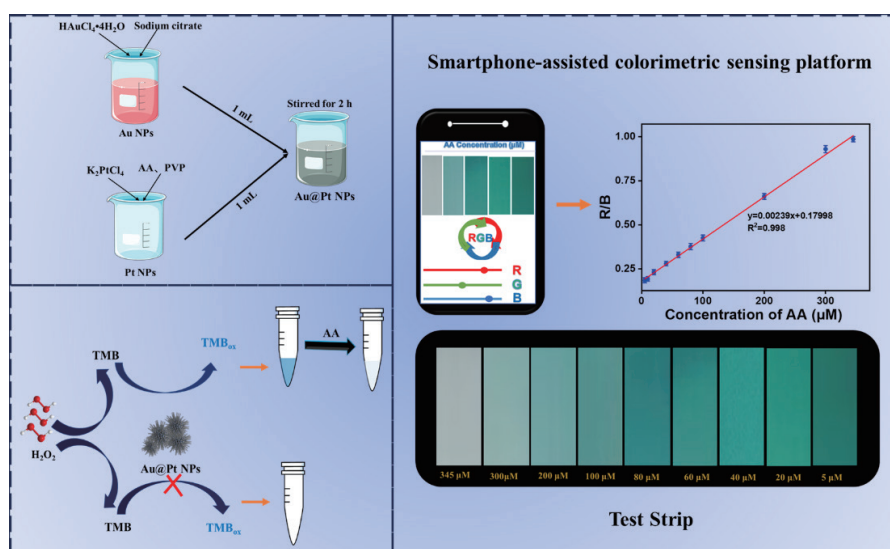


Fig. 1. (Color online) Schematic illustration of colorimetric detection of AA using Au@Pt nanozymes.

analysis by yielding more detailed data. Furthermore, the sensor exhibits strong selectivity and dependability, and it has been effectively utilized for extensive AA detection in fruits. The colorimetric sensor offers a new, easy-to-use, and effective approach for AA analysis that is free of pollution and capable of detecting specific substances.

2. Materials and Methods

2.1 Materials

$\text{HAuCl}_4 \cdot 4\text{H}_2\text{O}$, sodium borohydride (NaBH_4 , 95%), sodium citrate ($\text{Na}_3\text{C}_6\text{H}_5\text{O}_7 \cdot 2\text{H}_2\text{O}$, 99.5%), ascorbic acid (AA, 99%), poly(vinylpyrrolidone) (PVP, 98%), and K_2PtCl_4 were obtained from Macklin. Hydrogen peroxide (30% H_2O_2), TMB, triethylene glycol (TEG), and ascorbic acid (AA) were purchased from J&K Scientific Ltd. (Hefei, China). All the above reagents were analytically pure, and the solvent used was deionized water or absolute ethanol.

2.2 Instruments

The following instruments were used: scanning electron microscope (SEM, Zeiss Sigma 300), energy-dispersive spectrometer (EDS, Zeiss Sigma 300), X-ray diffractometer (XRD, Rigaku Ultima IV), and ultraviolet visible spectrophotometer (UV-vis diffraction, UV 5800 PC).

2.3 Preparation of Au NPs

Gold nanoparticles (Au NPs) were synthesized by controlling the ratio of $\text{HAuCl}_4 \cdot 4\text{H}_2\text{O}$ and sodium citrate concentrations. A solution of HAuCl_4 trihydrate (2 mL, 0.05 M) in water and 0.5 mL of 0.01 M sodium citrate in water was added to 40 mL of deionized water and stirred. Subsequently, 0.12 mL of freshly prepared 0.1 M NaBH_4 was added, resulting in a change in the color of the solution from colorless to red.

2.4 Preparation of Pt NPs

To synthesize Pt nanoparticles (Pt NPs), a K_2PtCl_4 solution was added to a mixture of AA and PVP. In a typical synthesis, a vial containing 8.0 mL of an aqueous solution with 10.5 mg of PVP and 6 mg of AA was preheated to 40 °C in an oil bath with magnetic stirring for 10 min. Then, 4.0 mL of an aqueous solution containing 9 mg of K_2PtCl_4 was added using a pipette. The reaction was allowed to continue at 40 °C for 5 min. The resulting product was collected by centrifugation, washed three times with water to remove PVP, and then redispersed in 15 mL of water.

2.5 Preparation of Au@Pt NPs

A 2 mL dispersion of Au NPs was mixed with a 2 mL dispersion of Pt NPs. The mixture was stirred for 2 h and then left to settle overnight at room temperature.

2.6 Peroxidase-like activity of Au@Pt NPs

The oxidase-like activity of Au@Pt NPs was evaluated through the peroxidase-like activity (POD-like activity) of TMB as a chromogenic substrate. Specifically, 30 μL of Au@Pt NPs (0.06 mg/L), 30 μL of the substrate (4 mM), and 90 μL of NaAc buffer (0.2 M, pH 4.0) were mixed and the absorption spectra were measured by UV-vis spectroscopy after a reaction at 37 $^{\circ}\text{C}$ for 20 min.

2.7 Colorimetric detection of AA and selectivity test

To test the sensitivity of AA in the Au@Pt NPs system, the following experiments were performed: under optimal conditions, 90 μL of NaAc buffer solution (0.2 M, pH 4.0), 30 μL of Au@Pt NPs (0.06 mg/L), 30 μL of TMB (2 mM), and 30 μL of H_2O_2 (6 mM) were reacted at 37 $^{\circ}\text{C}$ for 15 min. Then, different concentrations of AA were added to the above solution and incubated for 15 min, accompanied by distinct color changes from dark to light. Finally, changes in the absorbance spectra at 650 nm were recorded using the UV-vis spectrometer. At the same time, the color intensity of AA was examined using a smartphone under a stable light source and analyzed with the color identification app.

To verify the stability of the system, we added high concentrations of different kinds of metal ions, biological small molecules, and biological macromolecules to the system to carry out anti-interference experiments. Under optimal conditions, we choose the appropriate concentration of AA (300 μM) and the same concentration of interfering substances such as cations and biological small molecules (Fe^{3+} , Cu^{2+} , Ca^{2+} , K^+ , Mg^{2+} , Cys, Gly, Arg, His, and UA AA). After a sufficient reaction time, the absorbance at the wavelength of 650 nm was recorded. At the same time, the experimental results were photographed with a smartphone in a stable light source environment, then comprehensively analyzed with the color identification app.

2.8 AA analysis in real samples

First, we peeled kiwifruit and orange samples and ground the edible portion into a homogenate using a grinder. The above fresh fruit homogenate was put in a high-speed centrifuge and centrifuged at 12000 r/min for 20 min. Subsequently, to remove the insoluble component, the supernatants were filtered using a 0.20 μm syringe filter and diluted using ultrapure water. For AA detection, the diluted AA solution was added to the Au@Pt NP colorimetric system. N-Methylmaleimide was also added to remove the interference of sulfhydryl species. Then, the solutions were tested by UV-vis spectroscopy and with a smartphone in the RGB mode.

3. Results and Discussion

3.1 Synthesis and characterization of Au@Pt NPs

SEM imaging was employed to elucidate the morphology of Au@Pt NPs. As depicted in Fig. 2(a), the SEM image clearly revealed that the Au@Pt NPs show a core-shell configuration reminiscent of a nanoflower. The size of the Au@Pt NPs was around 70 nm. Smaller particles exhibited larger surface-area-to-volume ratios, providing more potential catalytic sites owing to the greater number of atoms on the surface. Additionally, the corresponding EDS spectrum [Fig. 2(f)] exhibited peaks corresponding to Au (20.69%) and Pt (17.55%), confirming the successful synthesis of Au@Pt NPs.

Furthermore, the wide-angle XRD pattern of the Au@Pt NPs is presented in Fig. 2(d). The pattern exhibits distinct peaks corresponding to the face-centered cubic crystal structure, specifically the (111), (200), (220), (311), and (222) planes. These peaks align with the characteristic peaks of Au (represented by the purple line, JCPDS 04-0783) and Pt (represented by the blue line, JCPDS 04-0802) in the database, confirming the presence of both metals in the Au@Pt NPs. The optical absorption spectra of the as-prepared Pt NPs, Au NPs, and Au@Pt NPs are shown in Fig. 2(e). A distinct peak at 269 nm, attributed to the presence of Pt NPs, is observed. Au NPs are known to exhibit a strong surface plasmon resonance (SPR) peak at 536 nm. In the case of Au@Pt NPs, both the Au SPR peak at 536 nm and the Pt NP peak at 269 nm are present. The appearance of these absorption peaks confirms the formation of core-shell bimetallic Au@Pt NPs.

3.2 Au@Pt NPs nanozyme activity study

The POD-like activity of Au@Pt NPs was investigated using a typical TMB oxidation reaction in the presence of H₂O₂. It is well established that peroxidase enzymes can catalyze the

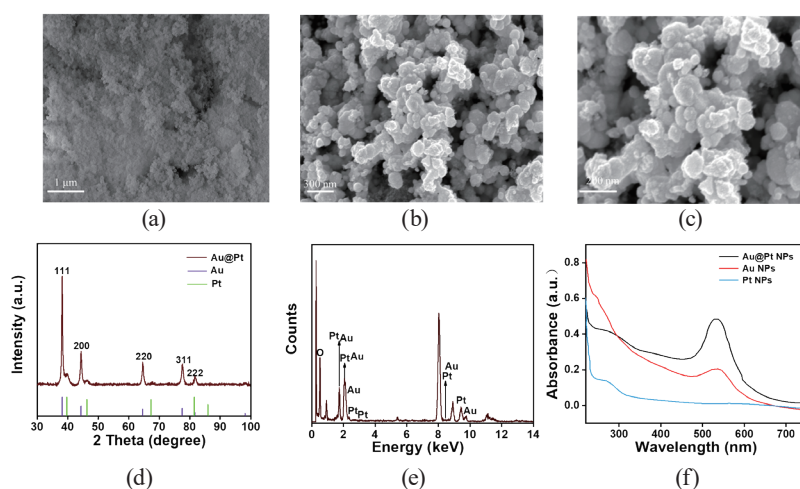


Fig. 2. (Color online) (a, b, c) SEM images of Au@Pt NPs, (d) XRD pattern, and (e) EDS and (f) optical absorption spectra of Au@Pt NPs.

oxidation of TMB, resulting in the formation of oxidized TMB and a characteristic absorption peak at 652 nm as well as a change in the color of the solution from colorless to blue. In Fig. 3(a), minimal changes in TMB_{ox} absorption were observed in the presence of Au@Pt NPs + TMB and other control groups. However, a significant absorption peak at 652 nm was observed in the group treated with H₂O₂-assisted Au@Pt NPs + TMB, accompanied by a change in the color of the solution from light yellow to blue. This observation indicates that Au@Pt NPs exhibit POD-like activity, enabling them to catalyze the production of oxidized substances when exposed to H₂O₂. Furthermore, in comparison with other nanozyme control groups (Au NPs + TMB + H₂O₂ and Pt NPs + TMB + H₂O₂), the catalytic activity of the Au@Pt NP nanozyme was found to be superior to all other groups.

The stronger the enzyme activity, the faster the enzymatic reaction. There are many factors affecting enzyme activity, mainly including enzyme concentration, pH, temperature, and reaction time. Therefore, the effects of pH (2.0–8.0), reaction temperature (2–60 °C), and time (5.0–45 min) on the POD-like activity were explored. It can be seen from the results that when the pH and temperature were 4.0 [Fig. 3(b)] and 25 °C [Fig. 3(d)], respectively, the highest catalytic activity was observed. After a reaction time of 25 min, the catalytic activity reached its peak [Fig. 3(c)]. Therefore, the highest POD-like activity of Au@Pt NPs was observed under the following experimental conditions: pH 4.0, 25 °C, and incubation for 25 min.

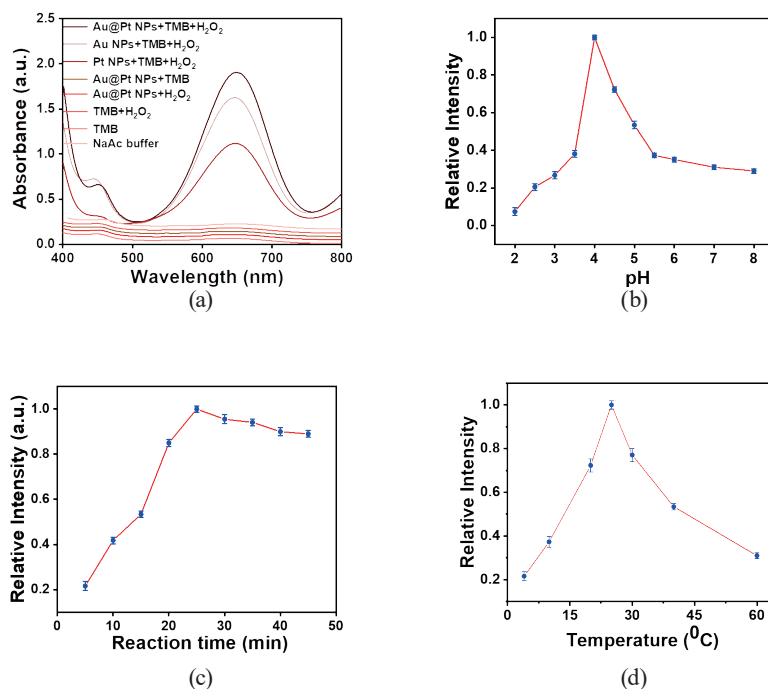


Fig. 3. (Color online) UV-vis absorption spectra of (a) Au@Pt NPs + TMB + H₂O₂, Au NPs + TMB + H₂O₂, Pt NPs + TMB + H₂O₂, Au@Pt NPs + TMB, Au@Pt NPs + H₂O₂, TMB + H₂O₂, TMB, and NaAc buffer. Effects of (b) pH, (c) reaction time, and (d) temperature on POD-like activity of Au@Pt NPs.

3.3 Colorimetric detection of AA

The detection performance of the colorimetric sensor using as-prepared Au@Pt NPs for AA analysis was studied under the optimal conditions. AA is a typical antioxidant with strong reducibility. If AA is present in the reaction system, the original blue color will fade significantly. Firstly, we investigate the viability of the Au@Pt NPs + TMB + H₂O₂ system in the catalysis of AA. As shown in Fig. 4(a), after adding AA to the Au@Pt NPs + TMB + H₂O₂ system, the blue color of the solution faded (inset II), accompanied by a significant decrease in absorbance (curve I). By studying the activity of the Au@Pt NP nanozyme, it can be proven that the Au@Pt NPs + TMB + H₂O₂ sensing system can be used for AA detection.

In Figs. 4(b) and 4(c), taking the AA concentration on the abscissa and $(A-A_0)/A_0$ on the ordinate (A: absorbance of AA measured at a certain concentration; A₀: blank control value), the absorbance of AA at 650 nm gradually decreases with the increase in AA concentration. Moreover, the proposed colorimetric platform for AA detection has good linearity in the range of 5–345 μM and a low LOD of 0.213 μM, indicating that the system has good detection performance for AA determination. After the calculation and fitting of the proposed sensor are shown to have good linear correlation, the regression equation is $y = 0.00238x + 0.16881$ ($R^2 = 0.998$). Compared with other approaches based on other nanozymes shown in Table 1, our fabricated sensor for AA assay shows a wider detection range and a lower LOD, indicating that this device has a certain practical significance in the detection of AA.

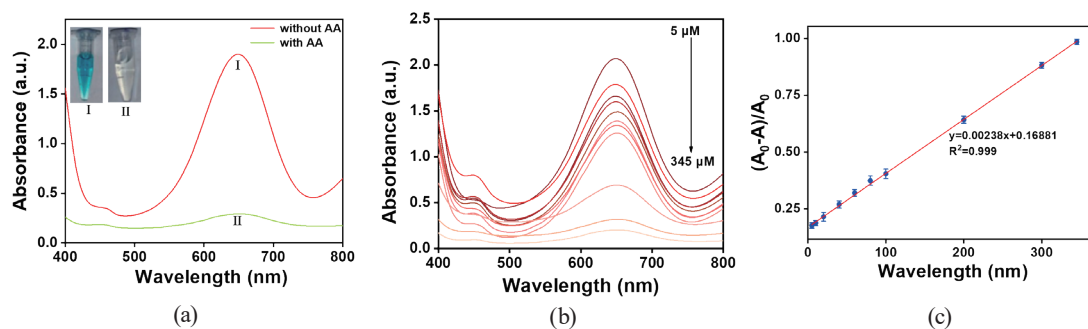


Fig. 4. (Color online) (a) UV-vis absorption spectra of Au@Pt NPs and TMB system (I) without and (II) with AA. Insets show the corresponding photographs. (b) UV-vis absorption spectra of AA. (c) Calibration curve of $(A_0-A)/A_0$ versus AA concentration.

Table 1

Method developed in this study and other published colorimetric detection methods for AA.

| Sensing probe | Method | Linear range (μM) | LOD (μM) | Reference |
|-------------------------------------|--------|-------------------|----------|-----------|
| Fe-N-C SANs | UV | 0.5–33 | 0.5 | (22) |
| Fe-N-C nanozyme | UV | 0.05–20 | 0.03 | (23) |
| NCNTs@MoS ₂ ^a | UV | 0.2–80 | 0.12 | (24) |
| MVCM ^b | UV | 20–500 | 3.57 | (24) |
| Au@Pt NPs | UV | 5–345 | 0.213 | This work |
| | RGB | | 0.706 | |

3.4 Detection of AA using smartphone in RGB mode

To enable a simpler and more portable on-site detection in a wider range of application scenarios, we have developed innovative AA visual quantitative test strips based on Au@Pt NPs. The test strips were prepared by spraying a solution of Au@Pt NPs (0.1 mg/mL), H₂O₂ (1.0 mM), and TMB (1.0 mM) onto acetate buffer solution (pH 4). Under visible light, the test strips exhibited a blue color. When AA was applied onto the surface of the test paper, a noticeable color change was observed with the naked eye after 10 min. As depicted in Fig. 5(a), different concentrations of AA caused distinguishable color changes (this paper is glass test paper with a size of 2 × 2 cm²). To achieve on-site and visual monitoring, we combined the portable test strip with the accurate color recognition function of a smartphone. Initially, the smartphone camera captures images of the Au@Pt NP test paper. Subsequently, software (color identification) I recognizes the colors in the acquired images and converts them into red (R), green (G), and blue (B) values. To ensure the accuracy of the method, we established a linear relationship between the AA concentration on the test paper (abscissa) and the ratio of R to B (R/B) (ordinate) for AA quantitative detection.

As shown in Fig. 5(b), R/B and AA concentrations (5 to 345 μM) exhibited a good linear relationship, and the linear regression equation was $y = 0.00239x + 0.17988$ ($R^2 = 0.99$) with the LOD of 0.706 μM. These data prove that the smartphone-aided sensing platform could achieve an efficient and highly sensitive AA detection.

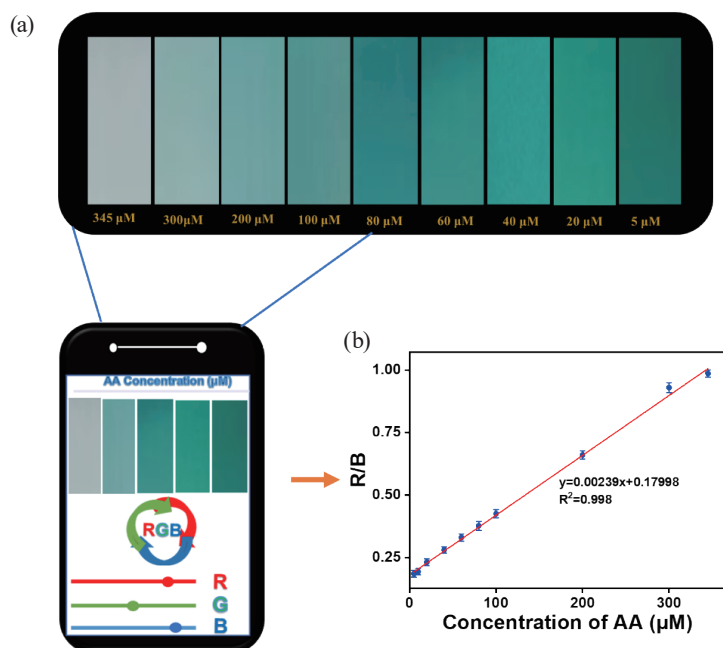


Fig. 5. (Color online) (a) Image of sensing test paper for different concentrations of AA after reaction in visible light. (b) Plot of relative color information (R/B) versus concentration of AA on the test paper

3.5 Selectivity of AA assay

To study the interference resistance of colorimetric sensors, different interfering ions (Fe^{3+} , Cu^{2+} , Ca^{2+} , K^+ , Mg^{2+} , Cys, Gly, Arg, His, and UA AA) were added under the optimal reaction conditions. The results are shown in Fig. 6(a). It can be seen that the colors of the other solutions were basically unchanged. Among the many kinds of ions and amino acids, the sensing system has good selectivity to AA and the best response to AA. Therefore, we can build an AA detection colorimetric sensing platform based on the Au@Pt NP nanozyme.

3.6 Assay for real samples

AA has strong antioxidant capacity. For further verification of the practicality and credibility of the developed colorimetric sensors for AA detection, two common tropical fruits, kiwifruit and orange, were selected for actual sample testing. As shown in Fig. 6(b), the contents of AA in kiwifruit and orange were close to 15 and 4 mg/10 g in the UV-vis and RGB modes, respectively. The 2,2-diphenyl-1, -picrylhydrazyl (DPPH) method was also used to measure the total antioxidant capacity of AA in real samples. The results obtained by the DPPH method (kiwifruit: 15 mg/10 g; orange: 4 mg/10 g) were in fair agreement with those of our established strategy. In addition, the *RSD* values of our method for all real samples were less than 5% compared with the results of the DPPH method, as shown in Table 2, indicating that the Au@Pt NPs + TMB + H_2O_2 system has strong reliability in the determination of the AA content in tropical fruits and broad development prospects.

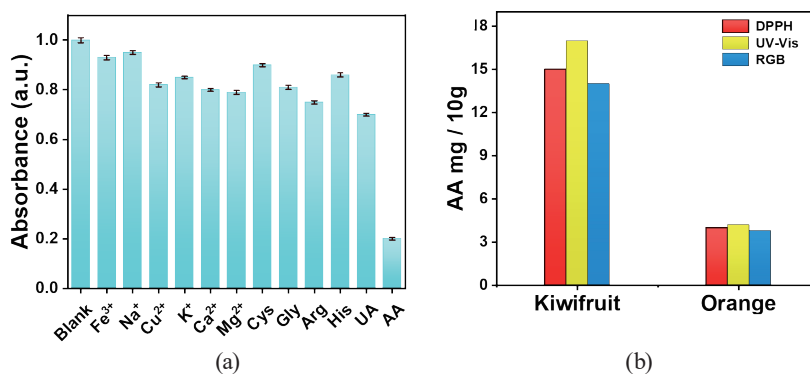


Fig. 6. (Color online) (a) Selectivity of the assay for AA over other potential interferences. The concentration of AA was 300 μM and that of other interferences was 300 μM . (b) Detection of AA in kiwifruit and orange using UV-vis spectrometer, smartphone modes, and DPPH method.

Table 2
Results of our method and DPPH method for AA in real samples.

| Sample | DPPH (mg/10 g) | UV-vis (mg/10 g) | RSD (%) | RGB (mg/10 g) | RSD (%) |
|-----------|-------------------|---------------------|---------|------------------|---------|
| Kiwifruit | 15.01 | 17.05 | 2.476 | 14 | 4.869 |
| Orange | 4.02 | 4.203 | 2.157 | 3.805 | 4.072 |

4. Conclusion

The prepared Au@Pt NP nanozymes showed excellent POD-like properties due to their unique structural characteristics, and a new colorimetric detection method for AA was constructed. At the same time, a smartphone auxiliary sensing platform was developed by combining colorimetric test paper with a smartphone, which realized a convenient and rapid detection of AA in fruit samples. The results show that the colorimetric detection method and integrated test strip have the advantages of high sensitivity, good selectivity, and good stability in the detection of AA, which proves the viability of the smartphone-assisted sensing platform, which is expected to become an ideal detection tool for vitamin C in fruits and other foods.

Acknowledgments

This work was supported by the Natural Science Foundation of the Anhui Higher Education Institutions of China (nos. 2022AH051118, 2022AH051110, and 2022AH051085).

References

- 1 M. Arabi and L. Chen: *Langmuir* **38** (2022) 5963. <https://pubs.acs.org/doi/abs/10.1021/acs.langmuir.2c00935>
- 2 Y. Ding, M. Zhao, J. Yu, Z. Li, X. Zhang, Y. Ma, H. Li, and S. Chen: *Talanta* **219** (2020) 121299. <https://pubmed.ncbi.nlm.nih.gov/32887041/>
- 3 P. J. O'Connell, C. Gormally, M. Pravda, and G. G. Guilbault: *Analytica Chimica Acta*. **431** (2001) 239. <https://www.sciencedirect.com/science/article/abs/pii/S0003267000013301>
- 4 E. Campbell, M. Vissers, C. Wohlrab, K. Hicks, M. Strother, B. Robinson, S. Bozonet, and G. Dachs: *Free Radical Biology and Medicine* **100** (2016) 132. <https://www.sciencedirect.com/science/article/abs/pii/S0891584916308176>
- 5 X. Huang, M. Jiang, H. Zeng, J. Wu, J. Wu, X. Liu, L. Zhou, and Y. Yuan: *Materialstoday* **36** (2023) 106775. <https://www.sciencedirect.com/science/article/abs/pii/S2352492823014666>
- 6 A. Duarte-Sierra, M.E. Tiznado-Hernández, D. K. Jha, N. Janmeja, and J. Arul: *Comprehensive Reviews in Food Sci. Food Safety* **19** (2020) 3659. <https://ift.onlinelibrary.wiley.com/doi/abs/10.1111/1541-4337.12628>
- 7 V. Gökmen, N. Kahraman, N. Demir, and J. Acar: *J. Chromatogr. A* **881** (2000) 309. <https://www.sciencedirect.com/science/article/abs/pii/S0021967300000807>
- 8 L. Yang, B. Sun, H. Cui, L. Zhu, and G. Shan: *Int. J. Anal. Chem.* **2022** (2022) 3482759. <https://www.hindawi.com/journals/ijac/2022/3482759/>
- 9 Y. P. Dong, T. T. Gao, X. F. Chu, J. Chen, and C. M. Wang: *J. Lumin.* **154** (2014) 350. <https://www.sciencedirect.com/science/article/abs/pii/S0022231314002944>
- 10 Z. Wang, X. Teng, and C. Lu: *Analyst* **137** (2012) 1876. <https://pubs.rsc.org/en/content/articlelanding/2012/an/c2an00030j/unauth>
- 11 D. Kul, M. Emilia Ghica, R. Pauliukaite, and C. M. A. Brett: *Talanta* **111** (2013) 76. <https://www.sciencedirect.com/science/article/abs/pii/S0039914013001161>
- 12 Y. Zhang, P. Liu, S. Xie, M. Chen, M. Zhang, Z. Cai, R. Liang, Y. Zhang, and F. Cheng: *J. Electroanal. Chem.* **818** (2018) 250. <https://www.sciencedirect.com/science/article/abs/pii/S1572665718302534>
- 13 Y. Li, R. Javed, R. Li, Y. Zhang, Z. Lang, H. Zhao, X. Liu, H. Cao, and D. Ye: *Food Chem.* **406** (2023) 135017. <https://www.sciencedirect.com/science/article/abs/pii/S030881462202979X>
- 14 Q. Wang, Y. Ding, R. A. Dahlgren, Y. Sun, J. Gu, Y. Li, T. Liu, and X. Wang: *Anal. Chim. Acta* **1252** (2023) 341072. <https://www.sciencedirect.com/science/article/abs/pii/S0003267023002933>
- 15 R. Dadigala, R. Bandi, S.-Y. Han, and G.-J. Kwon: *Int. J. Biol. Macromol.* **234** (2023) 123657. <https://www.sciencedirect.com/science/article/abs/pii/S0141813023005500>
- 16 X. Feng, H. Fu, Z. Bai, P. Li, X. Song, and X. Hu: *New J. Chem.* **46** (2022) 239. <https://pubs.rsc.org/en/content/articlehtml/2021/nj/d1nj04491e>

- 17 M. Bilal and H. M. N. Iqbal: Coordination Chem. Rev. **388** (2019) 1. <https://www.sciencedirect.com/science/article/abs/pii/S0010854518305940>
- 18 M. L. Grilli: Metals **10** (2020) 820. <https://www.mdpi.com/2075-4701/10/6/820>
- 19 Z. Wu, C. Huang, Y. Dong, B. Zhao, and Y. Chen: Food Control **137** (2022) 108916. <https://www.sciencedirect.com/science/article/abs/pii/S0956713522001098>
- 20 J. Bonet-Aleta, J. I. García-Peiro, S. Irusta, and J. L. Hueso: Nanomaterials **12** (2022) 755. <https://www.mdpi.com/2079-4991/12/5/755>
- 21 W. Wang, Q. Luo, L. Li, S. Chen, Y. Wang, X. Du, and N. Wang: Adv. Compos. Hybrid Mater. **6** (2023) 139. <https://link.springer.com/article/10.1007/s42114-023-00718-0>
- 22 Z. Wang, R. Zhang, X. Yan, and K. Fan: Mater. Today **41** (2020) 81. <https://www.sciencedirect.com/science/article/abs/pii/S1369702120303011>
- 23 L. Zheng, F. Wang, C. Jiang, S. Ye, J. Tong, P. Dramou, and H. He: Coordination Chem. Rev. **471** (2022) 214760. <https://www.sciencedirect.com/science/article/abs/pii/S0010854522003551>
- 24 Y. Sun, B. Xu, X. Pan, H. Wang, Q. Wu, S. Li, B. Jiang, and H. Liu: Coordination Chem. Rev. **475** (2023) 214896. <https://www.sciencedirect.com/science/article/abs/pii/S001085452200491X>
- 25 C. Xia, W. He, X. F. Yang, P. F. Gao, S. J. Zhen, Y. F. Li, and C. Z. Huang: Anal. Chem. **94** (2022) 13440. <https://pubs.acs.org/doi/abs/10.1021/acs.analchem.2c02434>
- 26 L. Shen, M. A. Khan, X. Wu, J. Cai, T. Lu, T. Ning, Z. Liu, W. Lu, D. Ye, H. Zhao, and J. Zhang: Biosens. Bioelectron. **205** (2022) 114097. <https://www.sciencedirect.com/science/article/abs/pii/S0956566322001373>
- 27 W. Liu, L. Chu, C. Zhang, P. Ni, Y. Jiang, B. Wang, Y. Lu, and C. Chen: Chem. Eng. J. **415** (2021). <https://www.sciencedirect.com/science/article/abs/pii/S1385894721004708>

About the Authors



Laixin Gao received his B.Eng. and M.Eng. degrees from Anhui Polytechnic University, Wuhu, China, in 2010 and 2013, respectively. Since 2013, he has been with the College of Electrical Engineering, Chuzhou University, Chuzhou, China. His major research interests include sensor applications and nonlinear system control. (glx0411@126.com)



Lingchun Li received her B.Eng. and M.Eng. degrees from Anhui Polytechnic University, Wuhu, China, in 2008 and 2011, respectively. She received her Ph.D. degree at Nanjing Tech University, Nanjing, China, in 2021. Since 2011, she has been with the College of Electrical Engineering, Chuzhou University, Chuzhou, China. Her major research interests include nonlinear system control and packet dropouts. (lilingchun1985@126.com)

